www.nature.com/aps

Acta Pharmacologica Sinica

ARTICLE

Ruscogenin attenuates particulate matter-induced acute lung injury in mice via protecting pulmonary endothelial barrier and inhibiting TLR4 signaling pathway

Yu-wei Wang[1], Yun-hao Wu[1], Jia-zhi Zhang[1], Jia-hui Tang[1], Rui-ping Fan[1], Fang Li[1], Bo-yang Yu[1], Jun-ping Kou[1] and Yuan-yuan Zhang[1]

The inhalation of particulate matter (PM) is closely related to respiratory damage, including acute lung injury (ALI), characterized by inflammatory fluid edema and disturbed alveolar-capillary permeability. Ruscogenin (RUS), the main active ingredient in the traditional Chinese medicine *Ophiopogonis japonicus*, has been found to exhibit anti-inflammatory activity and rescue LPS-induced ALI. In this study, we investigated whether and how RUS exerted therapeutic effects on PM-induced ALI. RUS (0.1, 0.3, 1 $mg{\cdot}kg^{-1}{\cdot}d^{-1}$) was orally administered to mice prior to or after intratracheal instillation of PM suspension (50 mg/kg). We showed that RUS administration either prior to or after PM challenge significantly attenuated PM-induced pathological injury, lung edema, vascular leakage and VE-cadherin expression in lung tissue. RUS administration significantly decreased the levels of cytokines IL-6 and IL-1β, as well as the levels of NO and MPO in both bronchoalveolar lavage fluid (BALF) and serum. RUS administration dose-dependently suppressed the phosphorylation of NF-κB p65 and the expression of TLR4 and MyD88 in lung tissue. Furthermore, TLR4 knockout partly diminished PM-induced lung injury, and abolished the protective effects of RUS in PM-instilled mice. In conclusion, RUS effectively alleviates PM-induced ALI probably by inhibition of vascular leakage and TLR4/MyD88 signaling. TLR4 might be crucial for PM to initiate pulmonary lesion and for RUS to exert efficacy against PM-induced lung injury.

Keywords: ruscogenin; particulate matter; acute lung injury; bronchoalveolar lavage fluid; toll like receptor 4; endothelial permeability

Acta Pharmacologica Sinica (2021) 42:726–734; https://doi.org/10.1038/s41401-020-00502-6

INTRODUCTION

With the acceleration of industrialization and urbanization, air pollution has become a more serious problem that faces the whole world. Ambient particulate matter (PM), especially fine PM with an aerodynamic diameter less than 2.5 μm ($PM_{2.5}$), is the main component of air pollution [1]. In 2015, $PM_{2.5}$ ranked as the fifth greatest mortality risk factor, causing 4.2 million deaths worldwide [2]. Short-term exposure to PM_{10} and $PM_{2.5}$ is positively associated with respiratory mortality [3]. Therefore, there is an urgent need for the development of drugs to prevent and cure PM-derived damage to the body.

Inhaled PM is mostly deposited in the pulmonary region by sedimentation and diffusion [4, 5]. Environmentally derived free radicals carried by PM and the production of intracellular reactive oxygen species (ROS) induced by PM may contribute to inflammation, oxidative stress, genotoxicity, immune disorders, and apoptosis in lung tissue and multiple organs [6, 7]. The mortality rates of acute lung injury (ALI) and its more severe form, acute respiratory distress syndrome (ARDS), characterized by diffuse alveolar damage, alveolar epithelial, and vascular endothelial injury and protein-rich inflammatory edema fluid accumulation in the alveolar space, remain high at 30%–40% [8]. Low to moderate PM exposure increases the risk of ALI/ARDS development [9, 10]. Furthermore, PM has been confirmed to contribute to lung endothelial dysfunction and inflammation [7, 11]. In addition, inhibition of lung tissue inflammation attenuated PM-induced ALI [12–15].

Nuclear factor κB (NF-κB) is a ubiquitous modulator that regulates inflammation [16] and is closely related to inhaled pollutant-associated respiratory diseases [17]. Toll like receptor 4 (TLR4), the innate immune receptor of bacterial endotoxins, pathogen-associated molecular patterns (PAMPs) and danger-associated molecular patterns (DAMPs), plays a pivotal role in the induction of inflammatory responses [18, 19]. TLR4 activation leads to the phosphorylation of NF-κB p65 in a myeloid differentiation factor 88 (MyD88)-dependent or MyD88-independent manner, promoting the release of inflammatory cytokines [20]. TLR4 has been identified as a key functional protein in ALI [21]. Inhibition of TLR4 signaling and consequent inhibition of the inflammatory response ameliorated ALI triggered by various stimulants, such as lipopolysaccharide (LPS), intestinal ischemia-reperfusion, and viral infection [22–24]. When aspirated into the lung, PM releases both PAMPs and DAMPs, which are recognized by TLR4, mediating a pulmonary inflammatory response [25, 26].

[1]State Key Laboratory of Natural Products, Jiangsu Key Laboratory of TCM Evaluation and Translational Research, Department of Pharmacology of Chinese Material Medica, School of Traditional Chinese Pharmacy, China Pharmaceutical University, Nanjing 211198, China
Correspondence: Jun-ping Kou (junpingkou@cpu.edu.cn) or Yuan-yuan Zhang (yuanyuanzhang@cpu.edu.cn)
These authors contributed equally: Yu-wei Wang, Yun-hao Wu

Received: 29 April 2020 Accepted: 31 July 2020
Published online: 27 August 2020

Thus, TLR4 may be a target for the prevention and treatment of lung injury caused by air pollution.

Saponins and sapogenins, the main effective constituents of the traditional Chinese medicine *Ophiopogon japonicus*, exhibit anti-inflammatory, antitumor, antithrombotic, and antioxidant properties [27]. Ruscogenin (RUS), an active steroidal sapogenin in *O. japonicus*, was reported to significantly attenuate inflammation in LPS-induced ALI and monocrotaline-induced pulmonary arterial hypertension (PAH) by inhibiting NF-κB p65 activation [28, 29]. In vitro experiments also revealed the vital role of NF-κB in the anti-inflammatory function of RUS [30]. Additionally, RUS may exert endothelial regulatory properties [29, 31, 32]. Moreover, injection of the lyophilized Chinese herbal formula Yiqi Fumai, in which RUS is an effective compound, alleviated PM-challenged ALI mice via inhibition of TLR4 signaling [14]. However, it remains unclear whether RUS attenuates PM-induced lung injury and its underlying mechanism.

In the present study, we aimed to further investigate the mechanism by which PM induces respiratory damage and contribute to the development of preventive and therapeutic drugs that protect against PM-induced injuries. The hypothesis that RUS attenuates PM-triggered ALI by suppressing pulmonary vascular leakage and the TLR4/MyD88 pathway was tested using a PM-induced ALI mouse model, and TLR4-knockout ($TLR4^{-/-}$) mice were used to verify the essential role of TLR4 in PM-induced ALI and the lung-protective property of RUS.

MATERIALS AND METHODS

Reagents and antibodies

RUS (505836) was purchased from J&K Scientific Ltd. (Beijing, China). Dexamethasone (DEX) (D1756) and Evans blue (E2129) were obtained from Sigma–Aldrich (St. Louis, MO, USA). Nitric oxide (NO), and ELISA kits for interleukin 6 (IL-6) (SBJ-M0044) and interleukin 1β (IL-1β) (SBJ-M0027) were provided by SenBeiJia Biological Technology Co., Ltd. (Nanjing, China). A myeloperoxidase (MPO) assay kit was purchased from Nanjing Jiancheng Bioengineering Institute (Nanjing, China). The primary antibodies anti-TLR4 (sc-293072), anti-MyD88 (sc-74532), and anti-p-NF-κB p65 (sc-166748) were purchased from Santa Cruz Biotechnology (Santa Cruz, CA, USA). Anti-NF-κB p65 (8242) was obtained from Cell Signaling Technology (Billerica, MA, USA). Anti-VE-cadherin antibody (ab33168) was obtained from Abcam (Cambridge, UK). The primary antibody anti-β-actin (AP0060) and secondary antibodies goat anti-rabbit IgG (H + L)-HRP (BS13278) and goat anti-mouse IgG (H + L)-HRP (BS12478) were provided by Bioworld Technology, Inc. (St. Louis Park, MN, USA).

PM preparation

An urban PM standard reference material (SRM) (1648a) collected in St. Louis, MO, USA, was obtained from the National Institute of Standards and Technology (NIST) (Gaithersburg, MD, USA). The PM was suspended in phosphate-buffered saline (PBS) to a final concentration of 25 mg/mL and ultrasonicated for 30 min before administration.

Animal care

Male ICR mice (18–22 g) were provided by the Experimental Animal Center of Yangzhou University (certificate number: SCXK Jiangsu 2017-0007). $TLR4^{-/-}$ and control (WT) mice were obtained from the Nanjing Biomedical Research Institute of Nanjing University (certificate number: SCXK Jiangsu 2018-0008). All mice were maintained at 25 °C with a 12 h light/12 h dark cycle and given free access to food and water. Animal welfare was ensured, the animal experimental procedures were in accordance with the National Institutes of Health Guide for the Care and Use of Laboratory Animals, and all experimental protocols were approved by the Animal Ethics Committee of China Pharmaceutical University.

Experimental design and PM exposure

After 3 days of adaptive feeding, the ICR mice were randomly divided into six groups ($n = 6$): the sham operation (sham) group, model group, model + RUS (0.1, 0.3, and 1 mg/kg) groups and DEX (1 mg/kg) group. WT and $TLR4^{-/-}$ mice were divided into six groups ($n = 6$) as follows: the WT group, WT + model group, WT + model + RUS (1 mg/kg) group, $TLR4^{-/-}$ group, $TLR4^{-/-}$ + model group and $TLR4^{-/-}$ + model + RUS (1 mg/kg) group. The mice in the model group received 40 μL (50 mg/kg) of a PM suspension by intratracheal instillation as previously described [14], while mice in the control groups received an equal volume of sterile PBS. RUS and DEX were administered orally 1 h prior to PM treatment. To determine the therapeutic role of RUS, ICR mice were divided into six groups ($n = 6$): the sham group; model group; and model + RUS (1 mg/kg) groups, which were administered RUS at 1, 3, 6, and 12 h after PM instillation. Mice were euthanized at 24 h after PM exposure, and serum, bronchoalveolar lavage fluid (BALF) and lung tissues were collected for subsequent experiments.

Histopathological analysis

Lung tissues fixed in 4% paraformaldehyde were embedded in paraffin, and 4-μm sections were deparaffinized and stained with hematoxylin and eosin (H&E). Pathological images were examined using an optical microscope (Nikon, Japan), and the extent of injury was scored by pathologists.

Lung wet/dry weight ratio

Lung tissues were weighed immediately after removal as the wet weight and then placed into an 80 °C oven for 48 h. The dried lung tissues were reweighed as the dry weight, and the wet/dry weight ratios were calculated.

Lung EB-albumin leakage

Mice were intravenously injected with EB-albumin (50 mg/kg) via the tail vein at 22 h after PM exposure and perfused 2 h later with PBS containing 5 mM EDTA-2Na on the right ventricle to remove the intravascular dye from the lung. Lung tissues were collected, flash frozen in liquid nitrogen and homogenized in a ten-fold volume of formamide. The homogenate was incubated at 60 °C for 18 h. After centrifugation at 5000 × *g* for 30 min, the absorption of EB in the supernatant was measured at 620 nm, and the EB content was measured with a standard curve.

Determination of the MPO, IL-1β, IL-6, and NO content

The MPO, IL-1β, IL-6, and NO content in the serum and BALF was determined using assay kits according to the corresponding manufacturer's instructions.

Lung immunohistochemistry

After the standard protocol described above prior to H&E staining was carried out, the sections were subjected to rehydration and antigen retrieval, incubated with hydrogen peroxide and blocked. The sections were first incubated with primary antibody against TLR4 (1:200 dilution, Santa Cruz Biotechnology, USA) at 4 °C overnight. Secondary antibodies and diaminobenzidine were added according to the manufacturer's instructions (Bioworld, USA). Finally, images of representative fields were captured with Leica QWin Plus version 3 software (Leica Microsystems, Cambridge, UK). The integrated optical density of the positive staining area was measured using Image-Pro Plus 5.1 (Media Cybernetics, Rockville, MD, USA), and protein expression levels are expressed as the average optical density.

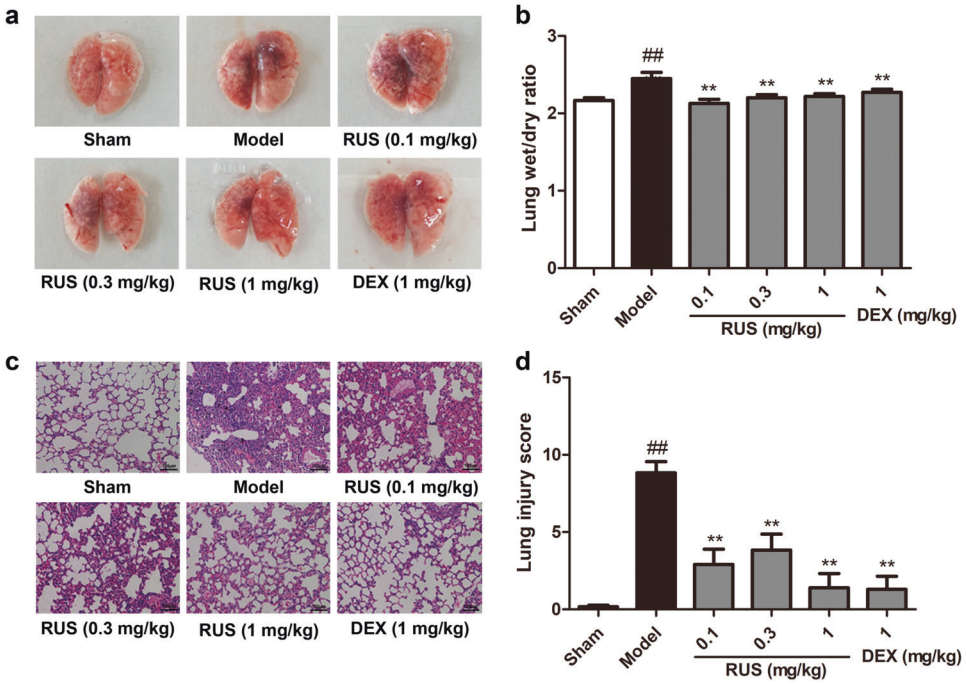

Fig. 1 RUS ameliorated PM-induced pulmonary pathological damage in mice. Mice were orally administered RUS (0.1, 0.3, 1 mg/kg) or DEX (1 mg/kg) prior to intratracheal PM (50 mg/kg) injection, and lung tissues were collected at 24 h after PM challenge. **a** The gross morphology of the mouse lung was observed and recorded. **b** The lung wet/dry ratio was determined ($n = 6$ lung tissue samples from six mice). **c** Histopathological changes in the lung were measured by H&E staining (scale bar = 100 μm). **d** Lung pathological injury scores were calculated ($n = 3$ lung tissue samples from three mice). Data are shown as the means ± SDs. $^{\#\#}P < 0.01$ compared with the sham group; $^{**}P < 0.01$ compared with the model group.

Western blot analysis

Lung tissues were homogenized in cold RIPA buffer (Beyotime, Haimen, China). The total protein in lung tissues was quantified using a BCA protein assay kit (Beyotime, Haimen, China). Equal amounts of total protein (30 μg) in each group were separated on SDS-PAGE gels and subsequently transferred to PVDF membranes (Merck Millipore, Billerica, MA, USA). After being blocked in 5% BSA (BioFroxx, German) for 2 h, the immunoblots were incubated overnight at 4 °C with primary antibodies against the following: VE-cadherin (1:1000 dilution, Abcam, UK), TLR4, MyD88, p-NF-κB p65 (1:200 dilution, Santa Cruz Biotechnology, USA), NF-κB p65 (1:1000 dilution, Cell Signaling Technology, USA), and β-actin (1:10000, Bioworld, USA). After washing three times with TBST, the membranes were incubated with IgG (H + L)-HRP secondary antibodies for 1.5 h at room temperature. Bands were detected using an ECL kit (Vazyme Biotechnology, Nanjing, China) and analyzed with Image Lab software 5.2 (Bio-Rad, Hercules, CA, USA).

Statistical analysis

Data are expressed as the means ± standard deviations (SDs). Statistical significance was estimated by one-way analysis of variance (ANOVA) followed by Dunnett's or Tukey's test using GraphPad Prism version 5.0 software (GraphPad Software, San Diego, CA, USA). A *P*-value <0.05 indicated a statistically significant difference.

RESULTS

RUS ameliorated pulmonary pathological damage in PM-induced ALI in mice

The lung tissues of mice in the model group exhibited massive PM deposition, bleeding (Fig. 1a) and pulmonary edema (Fig. 1b), unlike those of mice in the sham group, but RUS at a range of doses (0.1, 0.3, 1 mg/kg) and DEX (1 mg/kg) ameliorated the extent of pulmonary injury and edema under PM exposure (Fig. 1a, b). Pathological lung tissues sections of mice from the model group showed a collapsed alveolar structure, the infiltration of inflammatory cells, thickening and inward folding of the bronchial epithelium and PM deposition in the pulmonary mesenchyme (Fig. 1c). Calculation of lung injury scores indicated the protective function of RUS against pulmonary lesions, and DEX showed a similar effect (Fig. 1d). Similarly, RUS (1 mg/kg) treatment clearly relieved PM-induced lung edema and histopathological damage when administered at 3, 6, and 12 h after PM instillation (Supplementary Fig. S1). Collectively, these findings show that RUS significantly improved pulmonary pathological damage in ALI initiated due to PM.

RUS protected the lung endothelial barrier in PM-triggered ALI in mice

Impaired pulmonary vascular endothelial barrier function is a typical pathological feature of ALI. A rapid increase in EB-albumin leakage in the lung tissues of model mice was observed, and this increase was downregulated via RUS and DEX treatment (Fig. 2a, b). In addition, suppressed VE-cadherin expression in the lung tissue of mice in the model group was reversed by RUS and DEX (Fig. 2c), suggesting that RUS and DEX maintained pulmonary endothelial permeability.

RUS attenuated pulmonary inflammation in PM-triggered ALI in mice

Furthermore, the effect of RUS on pulmonary inflammation stimulated by PM was examined. As shown in Fig. 3, RUS at three doses suppressed the levels of MPO (Fig. 3a, b), IL-1β (Fig. 3c, d), IL-6 (Fig. 3e, f), and NO (Fig. 3g, h) in both the BALF and serum, which were upregulated under PM treatment. In addition, RUS inhibited the phosphorylation of NF-κB p65 (Fig. 3i), a vital regulator of inflammation. Taken together, these results show that PM triggered a pulmonary inflammatory response under conditions of ALI, but RUS could protect lung tissues from inflammatory infiltration.

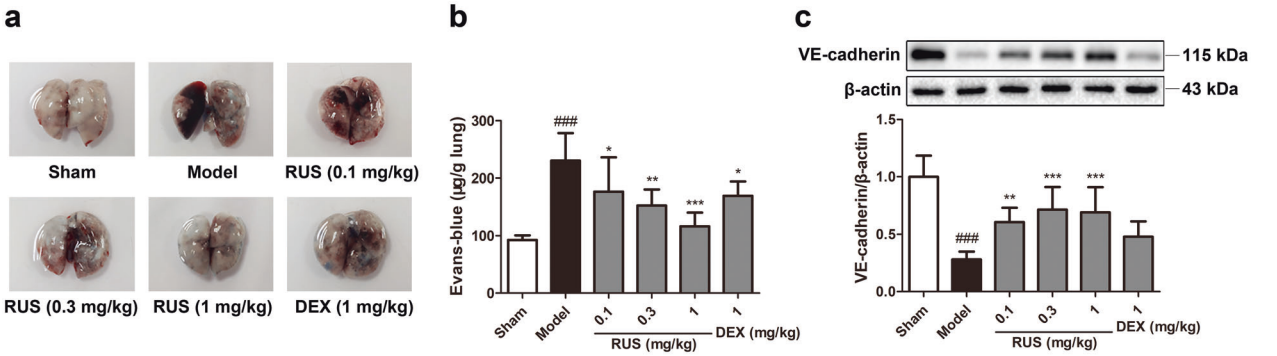

Fig. 2 RUS protected the lung endothelial barrier from PM exposure in mice. a The gross morphology of the mouse lung was recorded after EB-albumin injection. **b** The extravasation of EB-albumin dye into the lung parenchyma was determined ($n = 6$ lung tissue samples from six mice). **c** The expression of VE-cadherin in lung tissues was measured via Western blotting ($n = 3$ lung protein samples from three mice). Data represent the means ± SDs. $^{###}P < 0.001$ compared with the sham group; $^{*}P < 0.05$, $^{**}P < 0.01$, $^{***}P < 0.001$ compared with the model group.

RUS suppressed activated TLR4/MyD88 signaling in PM-challenged ALI mice

TLR4/MyD88 signaling was altered after PM challenge and was regulated by RUS. IHC and Western blot assays confirmed a remarkable increase in TLR4 levels in the lung tissues of model mice (Fig. 4a–c). This upregulation of TLR4 was reversed to some extent under RUS or DEX treatment in a dose-dependent manner (Fig. 4a–c), which corresponded with the expression of MyD88 (Fig. 4d). Thus, we suggest that PM activated TLR4/MyD88 signaling in lung tissues and that this activation was suppressed by RUS.

RUS failed to ameliorate pulmonary edema and pathological damage induced by PM in TLR4-knockout mice

To verify the hypothesis that TLR4 is essential in the effects of RUS in mitigating ALI provoked by PM, systemic TLR4$^{-/-}$ mice were utilized in subsequent experiments. TLR4$^{-/-}$ mice exhibited no significant lung tissue abnormalities when compared with WT mice (Fig. 5a). The TLR4$^{-/-}$ + model group exhibited less extensive pulmonary edema (Fig. 5b) and milder lung pathological injury than the WT + model group (Fig. 5c, d). Interestingly, TLR4 knockout diminished the RUS-mediated improvement in pulmonary lesions under PM exposure (Fig. 5a–d). These data suggest that RUS alleviated PM-derived ALI in a TLR4 signaling pathway-dependent manner.

RUS failed to downregulate vascular permeability and NF-κB p65 and MyD88 expression in TLR4-knockout mice

In accordance with the pathological injury data, deletion of TLR4 partly decreased lung EB leakage after PM challenge and abolished VE-cadherin degradation, but RUS failed to rescue pulmonary vascular barrier dysfunction in the absence of TLR4 (Fig. 6a–c). To further elucidate the indispensable role of TLR4 in the effects of RUS treatment on PM-initiated ALI, the effect of RUS on NF-κB p65 phosphorylation and MyD88 expression in the lung tissues of TLR4$^{-/-}$ mice were also examined. As shown in Fig. 6d, e, in the TLR4$^{-/-}$ + model + RUS (1 mg/kg) group, the levels of MyD88 and p-NF-κB p65 were unchanged compared to those in the TLR4$^{-/-}$ + model group, indicating that deletion of TLR4 abrogated the PM-mediated increase and RUS-mediated inhibition of p-NF-κB p65 and MyD88 expression.

DISCUSSION

Persistent PM air pollution causes severe respiratory and systemic injury in many regions around the world, but the underlying mechanism remains unclear, and no efficient drugs or food supplements to prevent air pollution-derived injury have become available. The present study demonstrated that RUS significantly attenuated PM-induced ALI in mice. RUS efficiently inhibited lung edema, lung injury, vascular leakage, inflammatory cytokine release, and the activation of TLR4 signaling under PM challenge. The essential role of TLR4 in the toxic pulmonary effect of PM and therapeutic effect of RUS on PM-triggered pulmonary lesions was also confirmed. Knockout of TLR4 partly prevented PM-induced damage to lung tissue and eliminated the protective effect of RUS. Our data suggest that TLR4 is the main receptor by which PM induces lung injury and that TLR4 plays an important role in the pulmonary protective effect of RUS.

The respiratory system is the initial component of the body attacked by inhaled PM and is subjected to direct attack. Increases in daily PM_{10} and $PM_{2.5}$ concentrations of 10 μg/m^3 are associated with increases in daily respiratory mortality of 0.47% and 0.74%, respectively [33]. Ultrafine PM can reach extrapulmonary organs and cause systemic diseases as the result of damage to the air–blood barrier of lung tissue [34, 35]. Thus, the prevention of PM-induced lung injury is of great significance for systemic protection against air pollutants.

As PM varies geographically and with the seasons [36], we applied an urban PM SRM (1648a) to stimulate the effects of PM in this study, which had the advantages of high stability and repeatability and has been previously applied by intratracheal instillation in animal experiments [14, 37]. The mean diameter of PM from the SRM 1648a is ~5.85 μm [37], and when dispersed in PBS, the size of the PM ranges from 236.43 nm to 1.98 mm [38]. Furthermore, the specific morphological and chemical characteristics of the SRM 1648a have been described [14, 39].

Dysregulated inflammation and alveolar-capillary barrier disruption are central pathophysiologic features in ALI and ARDS [40]. Inflammation, the typical response to lung injury induced by LPS or PM exposure in mouse models, is characterized by increased levels of cytokines, such as IL-6 and IL-1β, in BALF and serum [41, 42]. Pulmonary oxidative stress in response to inhaled PM is the leading cause of inflammation [43]. Levels of MPO, a pro-oxidant enzyme and indicator of neutrophil activation, in BALF or serum are positively related to challenge with environmental PM from various sources [44, 45]. NO, a biomarker of oxidative stress, was also found to be increased in lung tissue and serum in a mouse model exposed to PM [46, 47]. Activation of the NF-κB signaling pathway, a ubiquitous and pleiotropic modulator, by multiple stimulants regulated inflammation, the cell cycle and immunity [16]. Inhibition of the NF-κB pathway or its upstream transcription factors reduced the expression of proinflammatory cytokines in PM- or LPS-induced lung injury [48, 49]. In accordance with previous research, our present study confirmed the increased levels of IL-6, IL-1β, MPO, and NO in BALF and serum and the activation of NF-κB p65, indicating the pulmonary inflammatory

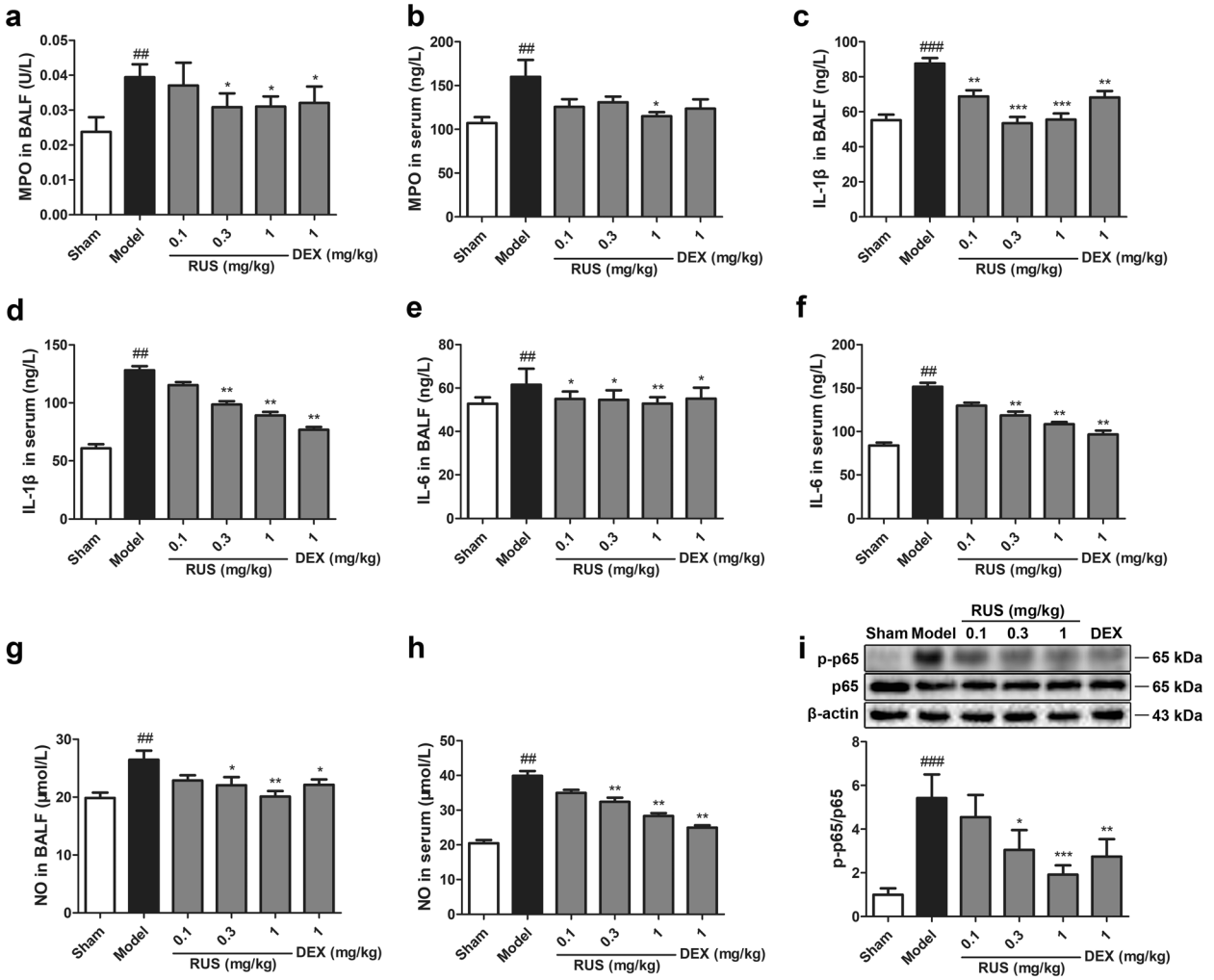

Fig. 3 RUS attenuated PM-triggered pulmonary inflammation in mice. a, **b** MPO levels in the BALF and serum were determined ($n = 6$ BALF or serum samples from six mice). **c**, **d** IL-1β levels in the BALF and serum were measured ($n = 6$ BALF or serum samples from six mice). **e**, **f** IL-6 levels in the BALF and serum were determined ($n = 6$ BALF or serum samples from six mice). **g**, **h** NO levels in the BALF and serum were measured ($n = 6$ BALF or serum samples from six mice). **i** Western blots and the p-p65 and p65 expression ratio ($n = 3$ lung protein samples from three mice). Data represent the means ± SDs. $^{\#\#}P < 0.01$, $^{\#\#\#}P < 0.001$ compared with the sham group; $^{*}P < 0.05$, $^{**}P < 0.01$, $^{***}P < 0.001$ compared with the model group.

response and oxidative stress, in PM-induced ALI model mice (Fig. 3). High cytokine levels can lead to alveolar-capillary barrier dysfunction by causing injury to epithelial or endothelial cells, contributing to pulmonary edema and hemorrhage in ALI [50]. Together, previous studies [13, 51] and our present research (Fig. 1b) verified the occurrence of pulmonary edema under PM exposure. The adherens junction (AJ) is the main component of the endothelial junction. VE-cadherin, also known as CDH5, is a dominant factor in the stability of AJs and plays a vital role in maintaining endothelial barrier integrity [52, 53]. According to a recent study, PM exposure elevated lung vascular permeability in vivo and downregulated the expression level of VE-cadherin in vitro [54]. Consistent with documented results, our data demonstrated that PM disrupted the pulmonary endothelial barrier, as indicated by the increased levels of EB-albumin leakage and suppressed VE-cadherin expression in lung tissue (Fig. 2).

TLR4 plays an important role in the PM-triggered inflammatory response. Previously published reports [14, 15, 55] and our present work (Fig. 4a–c) confirmed the upregulation of TLR4 in lung tissue under PM challenge. TLR4 deficiency strongly suppressed the PM-induced inflammatory response [56, 57]. MyD88, the main signaling adapter of TLR4, is also crucial in PM-initiated inflammation. Knockout of MyD88 reduced the endocytosis of PM by neutrophils and suppressed the release of ROS and cytokines [58, 59]. In accordance with the above studies, our present work revealed that TLR4 deletion relieved lung injury (Fig. 5), supporting the key role of TLR4 in urban PM pollution-induced pulmonary diseases. In addition, our present study indicated the importance of TLR4 in inducing alveolar-capillary leakage and VE-cadherin downregulation in PM-triggered lung injury (Fig. 6a–c), further revealing the potential mechanism by which PM induces respiratory diseases.

RUS, a steroidal sapogenin first isolated from *Ruscus aculeatus* [60], was reported to inhibit LPS-induced ALI in mice and attenuate monocrotaline-induced PAH in rats [28, 29], indicating its ability to defend against pulmonary diseases. RUS has shown dominant anti-inflammatory activity in experimental models of lung damage [28, 29], cerebral ischemic injury [31, 61], diabetes [62], and nonalcoholic steatohepatitis [63]. Regarding its molecular mechanism, RUS inhibits the inflammatory response mainly by suppressing NF-κB signaling [28, 30, 60–62] and also suppresses the nucleotide-binding domain (NOD)-like receptor family, pyrin domain containing 3 (NLRP3), thioredoxin-interactive protein (TXNIP) [31] and protein kinase A (PKA)-dependent neutrophil

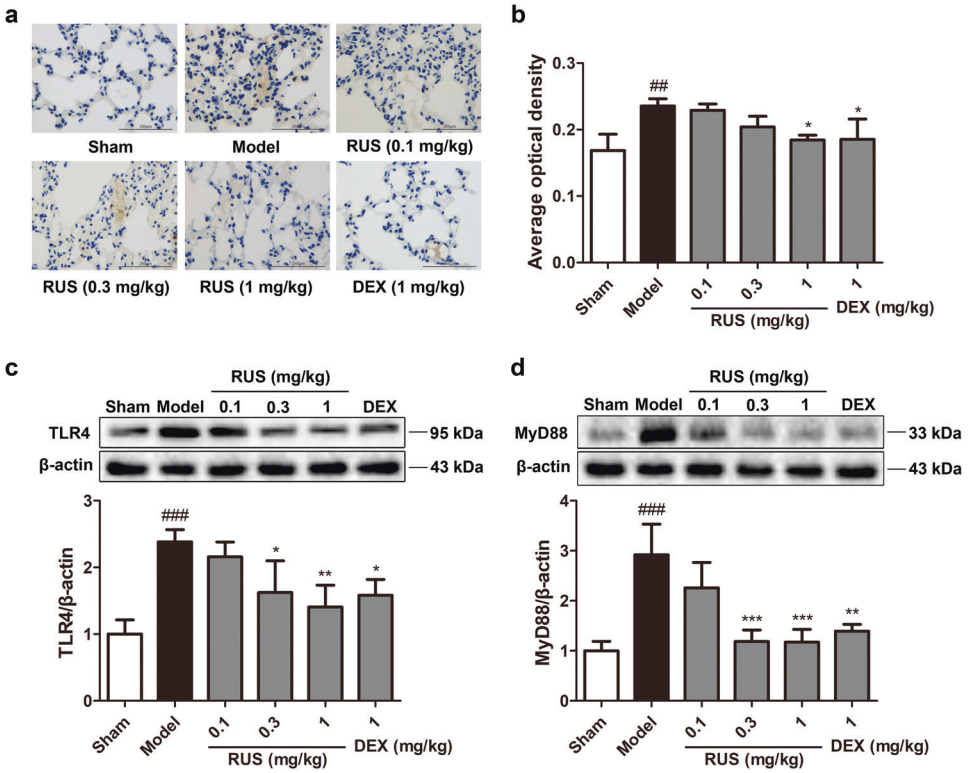

Fig. 4 RUS suppressed PM-induced activation of the TLR4/MyD88 signaling pathway in mice. a Typical immunohistochemical staining for TLR4 was observed in lung tissues (scale bar = 250 μm). **b** The average optical density from immunohistochemical staining was analyzed. The expression levels of TLR4 (**c**) and MyD88 (**d**) were determined by Western blot analysis. Data represent the means ± SDs ($n = 3$ lung protein samples from three mice). $^{\#\#}P < 0.01$, $^{\#\#\#}P < 0.001$ compared with the sham group; $^{*}P < 0.05$, $^{**}P < 0.01$, $^{***}P < 0.001$ compared with the model group.

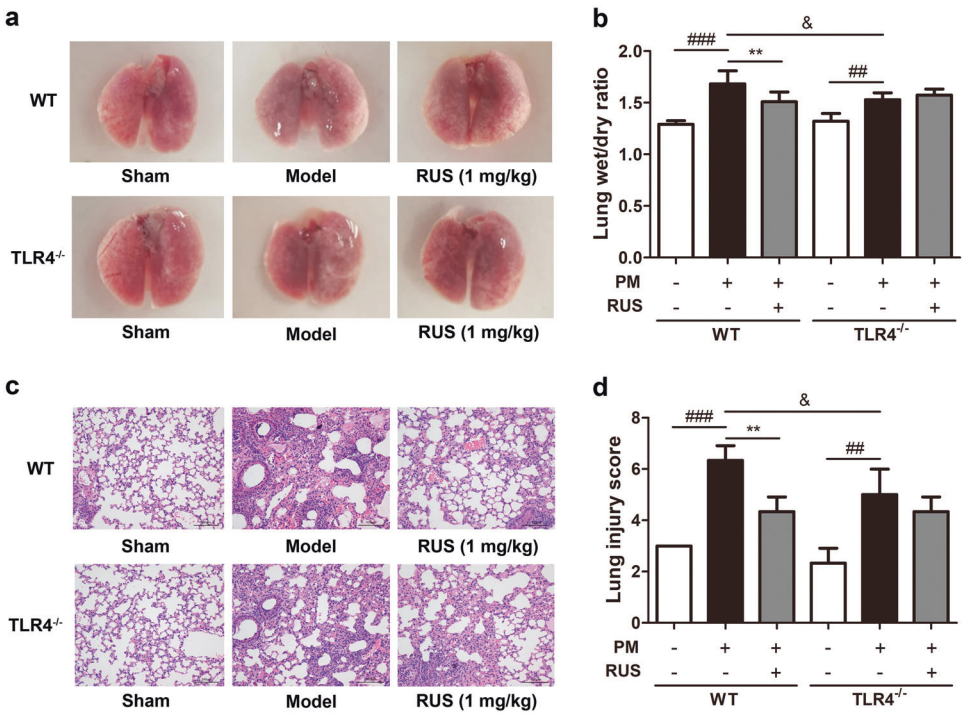

Fig. 5 RUS failed to ameliorate pulmonary edema and pathological damage induced by PM in TLR4-knockout mice. a The mouse lung morphology was recorded. **b** The lung wet/dry ratio was determined ($n = 6$ lung tissue samples from six mice). **c** Lung histopathological changes were measured by H&E staining (scale bar = 100 μm). **d** Lung pathological injury scores were calculated ($n = 3$ lung tissue samples from three mice). Data are shown as the means ± SDs. $^{\#\#}P < 0.01$, $^{\#\#\#}P < 0.001$ compared with the sham group; $^{**}P < 0.01$ compared with the model group; $^{\&}P < 0.05$ compared with the WT model group.

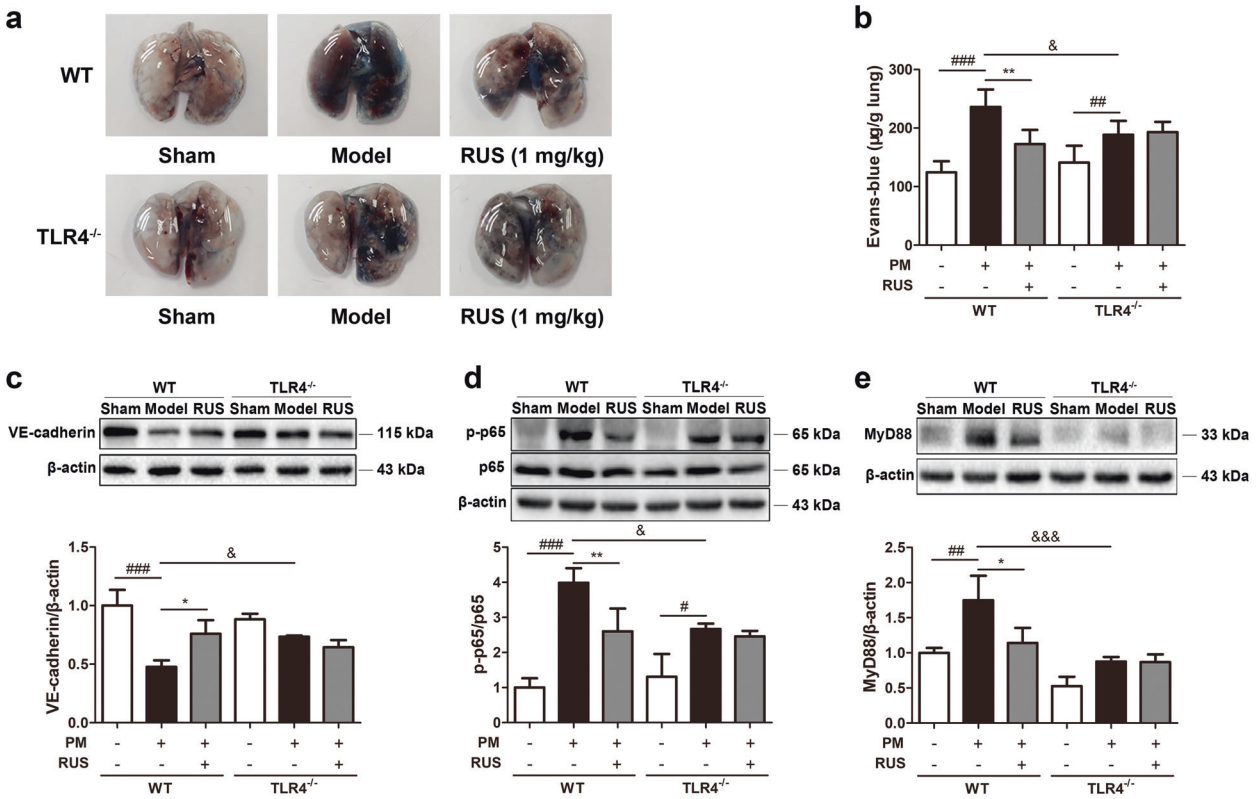

Fig. 6 RUS failed to decrease vascular permeability and NF-κB p65 and MyD88 expression in TLR4-knockout mice. a, **b** The extravasation of EB-albumin dye into the lung parenchyma was determined ($n = 6$ lung tissue samples from six mice). **c** The expression of VE-cadherin in lung tissues was measured via Western blot analysis ($n = 3$ lung protein samples from three mice). **d** Western blots and the ratio of p-p65 and p65 expression ($n = 3$ lung protein samples from three mice). **e** Western blot and the expression level of MyD88 ($n = 3$ lung protein samples from three mice). Data represent the means ± SDs. $^{\#\#}P < 0.01$, $^{\#\#\#}P < 0.001$ compared with the sham group; $^{*}P < 0.05$, $^{**}P < 0.01$ compared with the model group; $^{\&}P < 0.05$, $^{\&\&\&}P < 0.001$ compared with the WT model group.

activation [64]. In addition, RUS show activity against oxidative stress, according to previous studies [65, 66]. Decreases in MPO activity, the nitrate/nitrite content and NO synthase (iNOS) were observed in LPS-induced ALI mice after RUS treatment [28]. Similarly, our present work elucidated the pulmonary protective function of RUS against PM invasion via its activities against inflammation and oxidative stress, as demonstrated by the decreased levels of IL-6, IL-1β, MPO, and NO in BALF and serum and decreased NF-κB p65 phosphorylation (Fig. 3). In addition to the preventative property of RUS, we confirmed the dominant therapeutic effect of RUS against PM-induced lung injury by administering RUS at 3, 6, and 12 h after PM challenge (Supplementary Fig. S1). However, RUS failed to relieve lung injury shortly (1 h) after PM instillation, probably due to the poor condition of the mice after operation and reduced drug absorption.

RUS has been reported to inhibit the activated TLR4/MyD88/NF-κB signaling pathway in mice with LPS-induced ALI, while TLR4 was confirmed to be an upstream effector of RUS by its knockout [32]. In our study, RUS was also confirmed to block activated TLR4 signaling in a lung injury mouse model prepared by PM, further substantiating the molecular mechanism by which RUS defends against pulmonary injuries. In addition, although recent studies have revealed that some natural compounds and biomolecules alleviate PM-induced lung injury by inhibiting TLR4 signaling [67, 68], whether their pharmacodynamic effects are TLR4-dependent remains unclear. Our novel data show that RUS failed to ameliorate PM-induced lung injury (Figs. 5, 6a–c) and downstream MyD88 and NF-κB p65 activation (Fig. 6d, e) in the absence of TLR4, indicating that TLR4 is essential or even a potential target of RUS. Evidence shows that non-muscle myosin heavy chain IIA (NMMHC IIA) plays vital roles in various cellular physiological processes [69] and regulates TLR4 signaling in cerebral microvascular endothelial cells [70]. Furthermore, NMMHC IIA was identified as a specific RUS-binding protein [71]. NMMHC IIA mediates the anti-inflammatory and antithrombotic activities of saponin D39, a glycoside of RUS [72]. Thus, we speculate that RUS indirectly suppresses TLR4 signaling by directly interacting with NMMHC IIA and expect that this hypothesis will be further explored.

Furthermore, our data demonstrated that RUS restored PM-damaged lung endothelial barrier integrity by inhibiting the downregulation of VE-cadherin (Figs. 2c, 6c), similar to the documented vascular protective property of RUS against cerebral ischemic blood–brain barrier (BBB) dysfunction [31] and endothelial apoptosis in PAH [29] and LPS-induced lung injury [32]. Thus, in addition to its pulmonary protective and anti-inflammatory effects, RUS may regulate endothelial homeostasis, which deserves further investigation.

This study further addresses the potential mechanism by which PM induces respiratory diseases based on previous studies. With the use of TLR4$^{-/-}$ mice, TLR4 was identified as a vital molecule by which PM induces lung inflammation, oxidative stress and endothelial barrier dysfunction. The efficient protective property of RUS against PM-induced lung damage was confirmed, and the mechanism of RUS was investigated, which may provide inspiration for the use of traditional Chinese medicine and encourage investigation into the mechanisms by which air pollutants cause injury and protective measures against air pollutants. On the other hand, despite the accuracy and convenience of intratracheal

instillation, a model generated with this method would still be less clinically relevant than a mouse model generated by PM challenge via chronic inhalation. The definitive molecular mechanisms by which the specific components of PM induce pulmonary lesions and the signaling pathway by which PM induces the degradation of VE-cadherin remain to be further investigated. Finally, whether PM can lead to systemic organ and immune damage and drugs to improve these injuries deserve further research.

In summary, we first demonstrated that RUS, a natural compound with a prominent anti-inflammatory property, plays a protective role against PM-induced ALI, probably due to the inhibition of pulmonary vascular leakage and the TLR4 signaling pathway. TLR4 was found to be essential for the effect of RUS against PM-induced lung injury. The discoveries in this work may provide new insights into the treatment of PM-initiated injuries and therapeutic potential of RUS against air pollution-induced respiratory diseases.

ACKNOWLEDGEMENTS

This work was supported by the National Natural Science Foundation of China (No. 81773971) and the Double First-Class University Project of China Pharmaceutical University (CPU2018GF07).

AUTHOR CONTRIBUTIONS

YWW, JPK, and YYZ designed the project; YWW, YHW, JZZ, JHT, and RPF performed the experiments; YWW and YHW contributed to analyzing the data; YWW and RPF conducted the literature research; YWW organized the results and drafted the original manuscript; YWW, YHW, JPK, and YYZ reviewed and modified the manuscript; FL, BYY, JPK, and YYZ contributed to the funding acquisition.

ADDITIONAL INFORMATION

The online version of this article (https://doi.org/10.1038/s41401-020-00502-6) contains supplementary material, which is available to authorized users.

Competing interests: The authors declare no competing interests.

REFERENCES

1. Landrigan PJ, Fuller R, Acosta NJR, Adeyi O, Arnold R, Basu NN, et al. The lancet commission on pollution and health. Lancet. 2018;391:462–512.
2. Cohen AJ, Brauer M, Burnett R, Anderson HR, Frostad J, Estep K, et al. Estimates and 25-year trends of the global burden of disease attributable to ambient air pollution: an analysis of data from the global burden of diseases study 2015. Lancet. 2017;389:1907–18.
3. Liu L, Xia Z, Li J, Hu Y, Wang Q, Chen J, et al. Fibroblast growth factor 10 protects against particulate matter-induced airway inflammatory response through regulating inflammatory signaling and apoptosis. Am J Transl Res. 2019;11:6977–88.
4. Li D, Li Y, Li G, Zhang Y, Li J, Chen H. Fluorescent reconstitution on deposition of PM2.5 in lung and extrapulmonary organs. Proc Natl Acad Sci U S A. 2019;116:2488–93.
5. Deng Q, Deng L, Miao Y, Guo X, Li Y. Particle deposition in the human lung: health implications of particulate matter from different sources. Environ Res. 2019;169:237–45.
6. Feng S, Gao D, Liao F, Zhou F, Wang X. The health effects of ambient PM2.5 and potential mechanisms. Ecotoxicol Environ Saf. 2016;128:67–74.
7. Pope CA 3rd, Bhatnagar A, McCracken JP, Abplanalp W, Conklin DJ, O'Toole T. Exposure to fine particulate air pollution is associated with endothelial injury and systemic inflammation. Circ Res. 2016;119:1204–14.
8. Matthay MA, Zemans RL, Zimmerman GA, Arabi YM, Beitler JR, Mercat A, et al. Acute respiratory distress syndrome. Nat Rev Dis Prim. 2019;5:18. https://doi.org/10.1038/s41572-019-0069-0.
9. Reilly JP, Zhao Z, Shashaty M, Koyama T, Christie JD, Lanken PN, et al. Low to moderate air pollutant exposure and acute respiratory distress syndrome after severe trauma. Am J Respir Crit Care Med. 2019;199:62–70.
10. Li Y, Dong T, Jiang X, Wang C, Zhang Y, Li Y, et al. Chronic and low-level particulate matter exposure can sustainably mediate lung damage and alter CD4 T cells during acute lung injury. Mol Immunol. 2019;112:51–8.
11. Karki P, Meliton A, Sitikov A, Tian Y, Ohmura T, Birukova AA. Microtubule destabilization caused by particulate matter contributes to lung endothelial barrier dysfunction and inflammation. Cell Signal. 2019;53:246–55.
12. Lin CI, Tsai CH, Sun YL, Hsieh WY, Lin YC, Chen CY, et al. Instillation of particulate matter 2.5 induced acute lung injury and attenuated the injury recovery in ACE2 knockout mice. Int J Biol Sci. 2018;14:253–65.
13. Xu C, Shi Q, Zhang L, Zhao H. High molecular weight hyaluronan attenuates fine particulate matter-induced acute lung injury through inhibition of ROS-ASK1-p38/JNK-mediated epithelial apoptosis. Environ Toxicol Pharmacol. 2018;59:190–8.
14. Xia Y, S D, Jiang S, Fan R, Wang Y, Wang Y, et al. YiQiFuMai lyophilized injection attenuates particulate matter-induced acute lung injury in mice via TLR4-mTOR-autophagy pathway. Biomed Pharmacother. 2018;108:906–13.
15. Gu LZ, Sun H, Chen JH. Histone deacetylases 3 deletion restrains PM2.5-induced mice lung injury by regulating NF-κB and TGF-β/Smad2/3 signaling pathways. Biomed Pharmacother. 2017;85:756–62.
16. Panday A, Inda ME, Bagam P, Sahoo MK, Osorio D, Batra S. Transcription factor NF-κB: an update on intervention strategies. Arch Immunol Ther Exp (Warsz). 2016;64:463–83.
17. Traboulsi H, Guerrina N, Iu M, Maysinger D, Ariya P, Baglole CJ. Inhaled pollutants: the molecular scene behind respiratory and systemic diseases associated with ultrafine particulate matter. Int J Mol Sci. 2017;18:243.
18. Jiang D, Liang J, Li Y, Noble PW. The role of toll-like receptors in non-infectious lung injury. Cell Res. 2006;16:693–701.
19. Peri F, Piazza M. Therapeutic targeting of innate immunity with toll-like receptor 4 (TLR4) antagonists. Biotechnol Adv. 2012;30:251–60.
20. Kuzmich NN, Sivak KV, Chubarev VN, Porozov YB, Savateeva-Lyubimova TN, Peri F. TLR4 signaling pathway modulators as potential therapeutics in inflammation and sepsis. Vaccines (Basel). 2017;5:34. https://doi.org/10.3390/vaccines5040034.
21. Imai Y, Kuba K, Neely GG, Yaghubian-Malhami R, Perkmann T, van Loo G, et al. Identification of oxidative stress and toll-like receptor 4 signaling as a key pathway of acute lung injury. Cell. 2008;133:235–49.
22. Hsieh YH, Deng JS, Chang YS, Huang GJ. Ginsenoside Rh2 ameliorates lipopolysaccharide-induced acute lung injury by regulating the TLR4/PI3K/Akt/mTOR, Raf-1/MEK/ERK, and Keap1/Nrf2/HO-1 signaling pathways in mice. Nutrients. 2018;10:1208. https://doi.org/10.3390/nu10091208.
23. Yan J, Li J, Zhang L, Sun Y, Jiang J, Huang Y, et al. Nrf2 protects against acute lung injury and inflammation by modulating TLR4 and Akt signaling. Free Radic Biol Med. 2018;121:78–85.
24. Zhang R, Ai X, Duan Y, Xue M, He W, Wang C, et al. Kaempferol ameliorates H9N2 swine influenza virus-induced acute lung injury by inactivation of TLR4/MyD88-mediated NF-κB and MAPK signaling pathways. Biomed Pharmacother. 2017;89:660–72.
25. Tang Q, Huang K, Liu J, Wu S, Shen D, Dai P, et al. Fine particulate matter from pig house induced immune response by activating TLR4/MAPK/NF-κB pathway and NLRP3 inflammasome in alveolar macrophages. Chemosphere. 2019;236:124373.
26. Dai P, Shen D, Shen J, Tang Q, Xi M, Li Y, et al. The roles of Nrf2 and autophagy in modulating inflammation mediated by TLR4-NFκB in A549 cell exposed to layer house particulate matter 2.5 (PM 2.5). Chemosphere. 2019;235:1134–45.
27. Chen MH, Chen XJ, Wang M, Lin LG, Wang YT. Ophiopogon japonicus-a phytochemical, ethnomedicinal and pharmacological review. J Ethnopharmacol. 2016;181:193–213.
28. Sun Q, Chen L, Gao M, Jiang W, Shao F, Li J, et al. Ruscogenin inhibits lipopolysaccharide-induced acute lung injury in mice: involvement of tissue factor, inducible NO synthase and nuclear factor (NF)-κB. Int Immunopharmacol. 2012;12:88–93.
29. Bi LQ, Zhu R, Kong H, Wu SL, Li N, Zuo XR, et al. Ruscogenin attenuates monocrotaline-induced pulmonary hypertension in rats. Int Immunopharmacol. 2013;16:7–16.
30. Song J, Kou J, Huang Y, Yu B. Ruscogenin mainly inhibits nuclear factor-kappaB but not Akt and mitogen-activated protein kinase signaling pathways in human umbilical vein endothelial cells. J Pharmacol Sci. 2010;113:409–13.
31. Cao G, Jiang N, Hu Y, Zhang Y, Wang G, Yin M, et al. Ruscogenin attenuates cerebral ischemia-induced blood-brain barrier dysfunction by suppressing TXNIP/NLRP3 inflammasome activation and the MAPK pathway. Int J Mol Sci. 2016;17:1418.
32. Wu Y, Wang Y, Gong S, Tang J, Zhang J, Li F, et al. Ruscogenin alleviates LPS-induced pulmonary endothelial cell apoptosis by suppressing TLR4 signaling. Biomed Pharmacother. 2020;125:109868.
33. Liu C, Chen R, Sera F, Vicedo-Cabrera AM, Guo Y, Tong S, et al. Ambient particulate air pollution and daily mortality in 652 cities. N Engl J Med. 2019;381:705–15.
34. Li J, Li H, Li H, Guo W, An Z, Zeng X, et al. Amelioration of $PM_{2.5}$-induced lung toxicity in rats by nutritional supplementation with fish oil and vitamin E. Respir Res. 2019;20:76. https://doi.org/10.1186/s12931-019-1045-7.
35. Schraufnagel DE, Balmes JR, Cowl CT, De Matteis S, Jung SH, Mortimer K, et al. Air pollution and noncommunicable diseases: a review by the forum of international

respiratory societies' environmental committee, part 2: air pollution and organ systems. Chest. 2019;155:417–26.
36. González LT, Longoria-Rodríguez FE, Sánchez-Domínguez M, Leyva-Porras C, Acuña-Askar K, Kharissov BI, et al. Seasonal variation and chemical composition of particulate matter: a study by XPS, ICP-AES and sequential microanalysis using raman with SEM/EDS. J Environ Sci (China). 2018;74:32–49.
37. Xu XC, Wu YF, Zhou JS, Leyva-Porras C, Acuña-Askar K, Kharissov BI, et al. Autophagy inhibitors suppress environmental particulate matter-induced airway inflammation. Toxicol Lett. 2017;280:206–12.
38. Wang Y, Tang M. Integrative analysis of mRNAs, miRNAs and lncRNAs in urban particulate matter SRM 1648a-treated EA.hy926 human endothelial cells. Chemosphere. 2019;233:711–23.
39. Schantz MM, McGaw E, Wise SA. Pressurized liquid extraction of diesel and air particulate standard reference materials: effect of extraction temperature and pressure. Anal Chem. 2012;84:8222–31.
40. Matthay MA, Ware LB, Zimmerman GA. The acute respiratory distress syndrome. J Clin Invest. 2012;122:2731–40.
41. Chan YL, Wang B, Chen H, Ho KF, Cao J, Hai G, et al. Pulmonary inflammation induced by low-dose particulate matter exposure in mice. Am J Physiol Lung Cell Mol Physiol. 2019;317:L424–30.
42. Wu YX, He HQ, Nie YJ, Ding YH, Sun L, Qian F. Protostemonine effectively attenuates lipopolysaccharide-induced acute lung injury in mice. Acta Pharmacol Sin. 2018;39:85–96.
43. Rao X, Zhong J, Brook RD, Rajagopalan S. Effect of particulate matter air pollution on cardiovascular oxidative stress pathways. Antioxid Redox Signal. 2018;28:797–818.
44. Rückerl R, Schneider A, Hampel R, Breitner S, Cyrys J, Kraus U, et al. Association of novel metrics of particulate matter with vascular markers of inflammation and coagulation in susceptible populations -results from a panel study. Environ Res. 2016;150:337–47.
45. Farina F, Lonati E, Milani C, Massimino L, Ballarini E, Donzelli E, et al. In vivo comparative study on acute and sub-acute biological effects induced by ultrafine particles of different anthropogenic sources in BALB/c mice. Int J Mol Sci. 2019;20:2805.
46. Haberzettl P, Conklin DJ, Abplanalp WT, Bhatnagar A, O'Toole TE. Inhalation of fine particulate matter impairs endothelial progenitor cell function via pulmonary oxidative stress. Arterioscler Thromb Vasc Biol. 2018;38:131–42.
47. Li Y, Fu S, Li E, Sun X, Xu H, Meng Y, et al. Modulation of autophagy in the protective effect of resveratrol on $PM_{2.5}$-induced pulmonary oxidative injury in mice. Phytother Res. 2018;32:2480–6.
48. Wang J, Huang J, Wang L, Chen C, Yang D, Jin M, et al. Urban particulate matter triggers lung inflammation via the ROS-MAPK-NF-κB signaling pathway. J Thorac Dis. 2017;9:4398–412.
49. Ding YH, Song YD, Wu YX, He HQ, Yu TH, Hu YD, et al. Isoalantolactone suppresses LPS-induced inflammation by inhibiting TRAF6 ubiquitination and alleviates acute lung injury. Acta Pharmacol Sin. 2019;40:64–74.
50. Englert JA, Bobba C, Baron RM. Integrating molecular pathogenesis and clinical translation in sepsis-induced acute respiratory distress syndrome. JCI Insight. 2019;4:e124061. https://doi.org/10.1172/jci.insight.124061.
51. Cui A, Xiang M, Xu M, Lu P, Wang S, Zou Y, et al. VCAM-1-mediated neutrophil infiltration exacerbates ambient fine particle-induced lung injury. Toxicol Lett. 2019;302:60–74.
52. Gong H, Rehman J, Tang H, Wary K, Mittal M, Chaturvedi P, et al. HIF2α signaling inhibits adherens junctional disruption in acute lung injury. J Clin Invest. 2015;125:652–64.
53. Dong W, He B, Qian H, Liu Q, Wang D, Li J, et al. RAB26-dependent autophagy protects adherens junctional integrity in acute lung injury. Autophagy. 2018;14:1677–92.
54. Long YM, Yang XZ, Yang QQ, Clermont AC, Yin YG, Liu GL, et al. $PM_{2.5}$ induces vascular permeability increase through activating MAPK/ERK signaling pathway and ROS generation. J Hazard Mater. 2020;386:121659. https://doi.org/10.1016/j.jhazmat.2019.121659.
55. Xu M, Li F, Wang M, Zhang H, Xu L, Adcock IM, et al. Protective effects of VGX-1027 in $PM_{2.5}$-induced airway inflammation and bronchial hyperresponsiveness. Eur J Pharmacol. 2019;842:373–83.
56. Kampfrath T, Maiseyeu A, Ying Z, Shah Z, Deiuliis JA, Xu X, et al. Chronic fine particulate matter exposure induces systemic vascular dysfunction via NADPH oxidase and TLR4 pathways. Circ Res. 2011;108:716–26.
57. Bekki K, Ito T, Yoshida Y, Shah Z, Deiuliis JA, Xu X, et al. PM2.5 collected in china causes inflammatory and oxidative stress responses in macrophages through the multiple pathways. Environ Toxicol Pharmacol. 2016;45:362–9.
58. Shoenfelt J, Mitkus RJ, Zeisler R, Spatz RO, Powell J, Fenton MJ, et al. Involvement of TLR2 and TLR4 in inflammatory immune responses induced by fine and coarse ambient air particulate matter. J Leukoc Biol. 2009;86:303–12.
59. Miyake T, Wang D, Matsuoka H, Morita K, Yasuda H, Yatera K, et al. Endocytosis of particulate matter induces cytokine production by neutrophil via toll-like receptor 4. Int Immunopharmacol. 2018;57:190–9.
60. Huang YL, Kou JP, Ma L, Song JX, Yu BY. Possible mechanism of the anti-inflammatory activity of ruscogenin: role of intercellular adhesion molecule-1 and nuclear factor-kappaB. J Pharmacol. 2008;108:198–205.
61. Guan T, Liu Q, Qian Y, Yang H, Kong J, Kou J, et al. Ruscogenin reduces cerebral ischemic injury via NF-κB-mediated inflammatory pathway in the mouse model of experimental stroke. Eur J Pharmacol. 2013;714:303–11.
62. Lu HJ, Tzeng TF, Liou SS, Da Lin S, Wu MC, Liu IM. Ruscogenin ameliorates diabetic nephropathy by its anti-inflammatory and anti-fibrotic effects in streptozotocin-induced diabetic rat. BMC Complement Alter Med. 2014;14:110. https://doi.org/10.1186/1472-6882-14-110.
63. Lu HJ, Tzeng TF, Liou SS, Chang CJ, Yang C, Wu MC, et al. Ruscogenin ameliorates experimental nonalcoholic steatohepatitis via suppressing lipogenesis and inflammatory pathway. Biomed Res Int. 2014;2014:652680.
64. Lin YN, Jia R, Liu YH, Gao Y, Wang LL, Kou JP, et al. Ruscogenin suppresses mouse neutrophil activation: involvement of protein kinase A pathway. J Steroid Biochem Mol Biol. 2015;154:85–93.
65. Li F, Lv YN, Tan YS, Shen K, Zhai KF, Chen HL, et al. An integrated pathway interaction network for the combination of four effective compounds from ShengMai preparations in the treatment of cardio-cerebral ischemic diseases. Acta Pharmacol Sin. 2015;36:1337–48.
66. Li F, Zhang Y, Zeng D, Xia Y, Fan X, Tan Y, et al. The combination of three components derived from Sheng MaiSan protects myocardial ischemic diseases and inhibits oxidative stress via modulating MAPKs and JAK2-STAT3 signaling pathways based on bioinformatics approach. Front Pharmacol. 2017;8:21. https://doi.org/10.3389/fphar.2017.00021.
67. Jeong SY, Kim J, Park EK, Baek MC, Bae JS. Inhibitory functions of maslinic acid on particulate matter-induced lung injury through TLR4-mTOR-autophagy pathways. Environ Res. 2020;183:109230.
68. Liu L, Song C, Li J, Wang Q, Zhu M, Hu Y, et al. Fibroblast growth factor 10 alleviates particulate matter-induced lung injury by inhibiting the HMGB1-TLR4 pathway. Aging (Albany NY). 2020;12:1186–200.
69. Asensio-Juárez G, Llorente-González C, Vicente-Manzanares M. Linking the landscape of MYH9-related diseases to the molecular mechanisms that control non-muscle myosin II-A function in cells. Cells. 2020;9:E1458.
70. Lv Y, Liu W, Ruan Z, Xu Z, Fu L. Myosin IIA regulated tight junction in oxygen glucose-deprived brain endothelial cells via activation of TLR4/PI3K/Akt/JNK1/2/14-3-3ε/NF-κB/MMP9 signal transduction pathway. Cell Mol Neurobiol. 2019;39:301–19.
71. Yu BY, Kou JP, Huang YL, Jiang WW, Liu JH, inventors; Nanjing Suke Patent Agency Co. LTD, assignee. A potential drug target and its inhibitors for the prevention and treatment of cardio-cerebrovascular diseases related to inflammation. CN patent 101125146. 2008.
72. Zhai KF, Zheng JR, Tang YM, Li F, Lv YN, Zhang YY, et al. The saponin D39 blocks dissociation of non-muscular myosin heavy chain IIA from TNF receptor 2, suppressing tissue factor expression and venous thrombosis. Br J Pharmacol. 2017;174:2818–31.